

Understanding of magnetic behavior of the pseudo-binary $\text{Co}_{2-x}\text{Ni}_x\text{Zn}_{11}$: in the light of crystal and electronic structures

Amit Mondal[†], Sandip Kumar Kuila^{†,¶}, Rahul Pan^{†,¶}, Shubham Patel^{††}, Krishnendu Buxi[†], Subhadip Saha[†], Sivaprasad Ghanta[†], Maxim Avdeev^{†††}, Partha Pratim Jana^{†*}

([¶] equal contribution)

[†]Department of Chemistry, IIT Kharagpur, Kharagpur, 721302, India

^{††}Department of Physics, IIT Kharagpur, Kharagpur, 721302, India

^{†††} Australian Nuclear Science and Technology Organisation, New Illawarra Road, Lucas Heights, NSW 2234, Australia

^{†††} School of Chemistry, The University of Sydney, Sydney 2006, Australia

ppj@chem.iitkgp.ac.in

Supporting Information

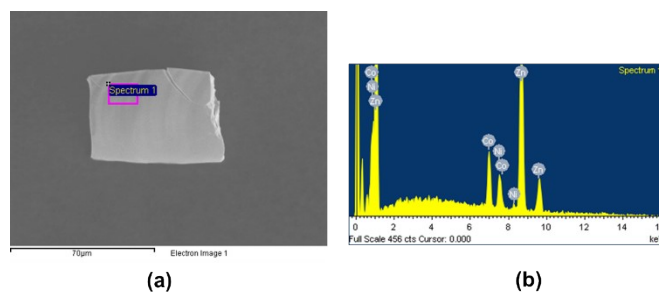


Fig. S1. (a) SEM image of the single crystal and (b) EDS spectrum of SC3 ($\text{Co}_{1.1}\text{Ni}_{0.9}\text{Zn}_{11}$).

Sample code	Loaded composition	Loaded composition (at. %)	EDS composition (at. %)
SC1	$\text{Co}_{1.7}\text{Ni}_{0.3}\text{Zn}_{11}$	$\text{Co}_{13.08}\text{Ni}_{2.30}\text{Zn}_{84.62}$	$\text{Co}_{13.10}\text{Ni}_{2.24}\text{Zn}_{84.66}$
SC2	$\text{Co}_{1.4}\text{Ni}_{0.6}\text{Zn}_{11}$	$\text{Co}_{10.77}\text{Ni}_{4.61}\text{Zn}_{84.62}$	$\text{Co}_{10.11}\text{Ni}_{4.40}\text{Zn}_{85.49}$
SC3	$\text{Co}_{1.1}\text{Ni}_{0.9}\text{Zn}_{11}$	$\text{Co}_{8.46}\text{Ni}_{6.92}\text{Zn}_{84.62}$	$\text{Co}_{8.32}\text{Ni}_{6.51}\text{Zn}_{85.17}$
SC4	$\text{Co}_{0.8}\text{Ni}_{1.2}\text{Zn}_{11}$	$\text{Co}_{6.15}\text{Ni}_{9.23}\text{Zn}_{84.62}$	$\text{Co}_{6.54}\text{Ni}_{9.72}\text{Zn}_{83.74}$
SC5	$\text{Co}_{0.5}\text{Ni}_{1.5}\text{Zn}_{11}$	$\text{Co}_{3.84}\text{Ni}_{11.54}\text{Zn}_{84.62}$	$\text{Co}_{3.42}\text{Ni}_{10.99}\text{Zn}_{85.59}$
SC6	$\text{Co}_{0.2}\text{Ni}_{1.8}\text{Zn}_{11}$	$\text{Co}_{1.53}\text{Ni}_{13.85}\text{Zn}_{84.62}$	$\text{Co}_{1.27}\text{Ni}_{13.04}\text{Zn}_{85.69}$

Table S1. Sample codes with their loaded composition and EDS composition.

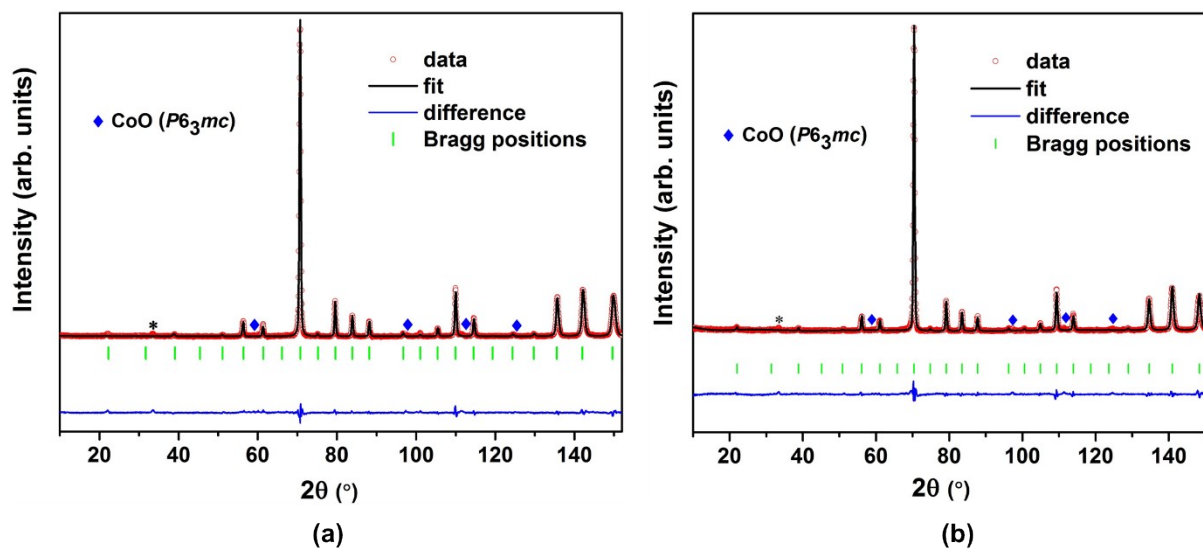
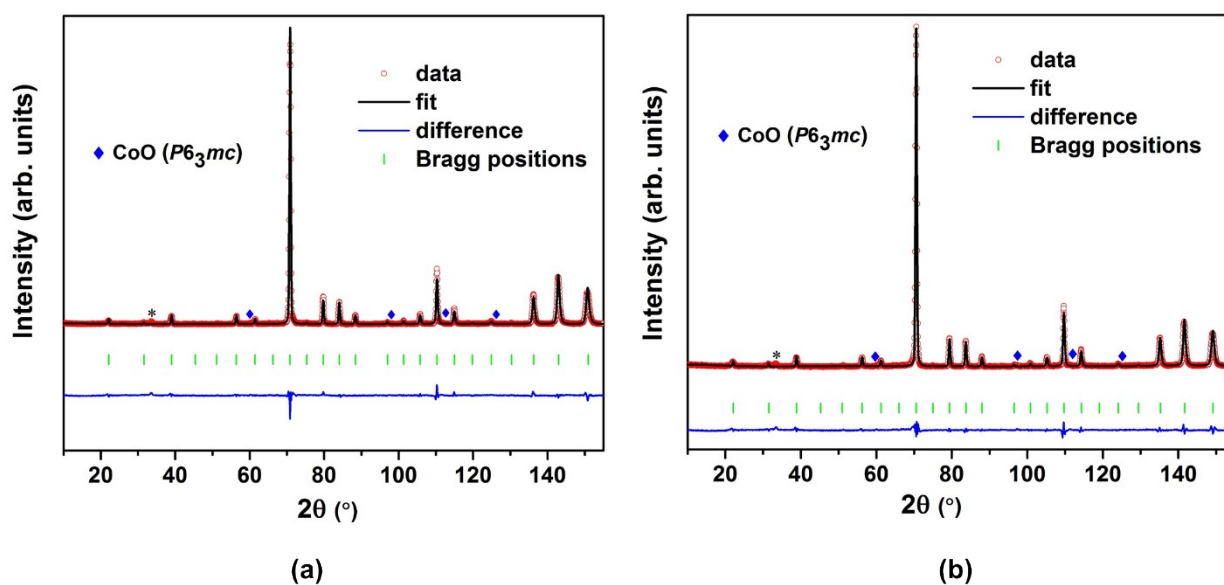


Fig. S2. Neutron powder diffraction data collected at (a) 3 K and (b) room temperature (300 K) for $\text{Co}_{1.1}\text{Ni}_{0.9}\text{Zn}_{11}$. The asterisks show $\sim 0.5\%$ of $\lambda/2$ harmonics.

Fig. S3. Neutron powder diffraction data collected at (a) 3 K and (b) room temperature (300 K) for $\text{Co}_{0.5}\text{Ni}_{1.5}\text{Zn}_{11}$. The asterisks show $\sim 0.5\%$ of $\lambda/2$ harmonics.



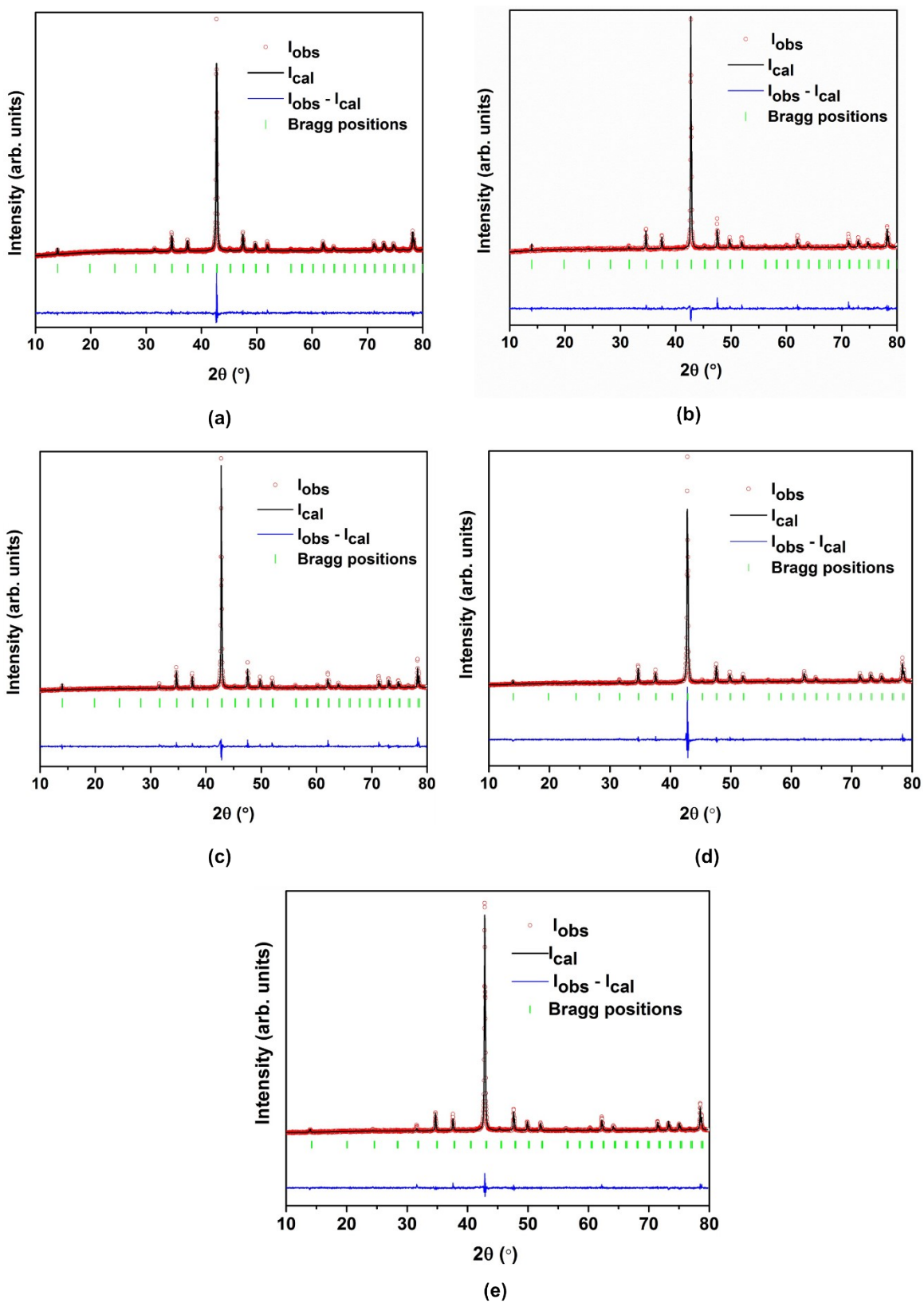


Fig. S4. Rietveld refinement plots for (a) $\text{Co}_{1.4}\text{Ni}_{0.6}\text{Zn}_{11}$, (b) $\text{Co}_{1.1}\text{Ni}_{0.9}\text{Zn}_{11}$, (c) $\text{Co}_{0.8}\text{Ni}_{1.2}\text{Zn}_{11}$, (d) $\text{Co}_{0.5}\text{Ni}_{1.5}\text{Zn}_{11}$, and (e) $\text{Co}_{0.2}\text{Ni}_{1.8}\text{Zn}_{11}$.

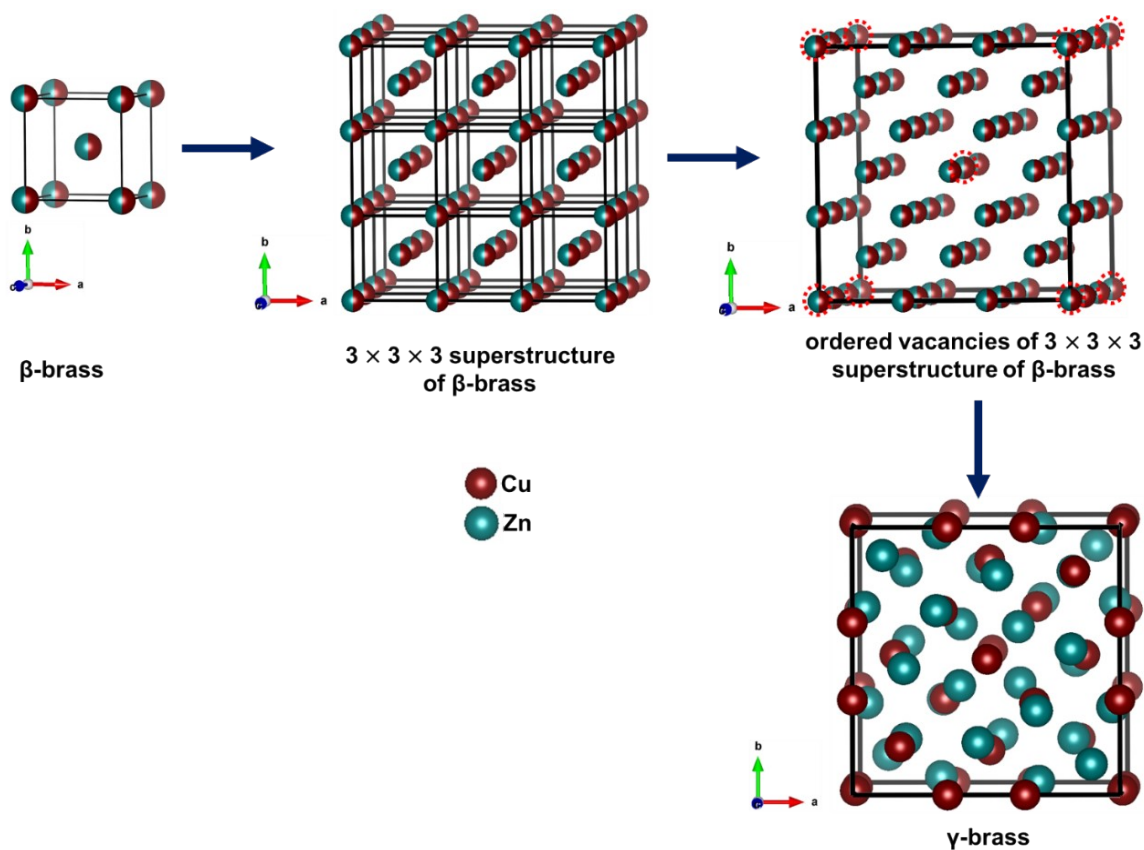


Fig. S5. Construction of γ -brass (Cu_5Zn_8) from β -brass (CuZn) structure.

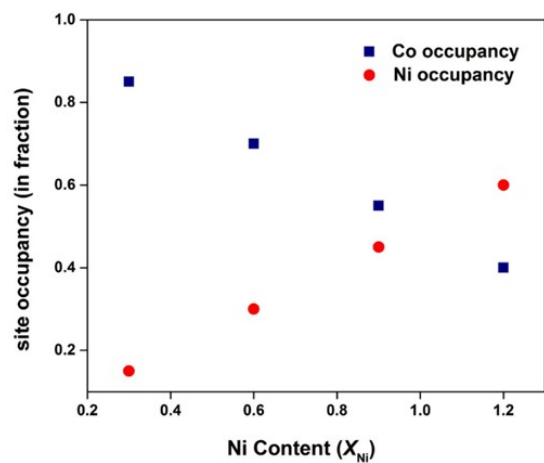


Fig. S6. Distribution pattern of Co and Ni at the OT ($8c$) site as a function of Ni content in $\text{Co}_2\text{-}_x\text{Ni}_x\text{Zn}_{11}$ suggested by SCXRD and EDS measurements.

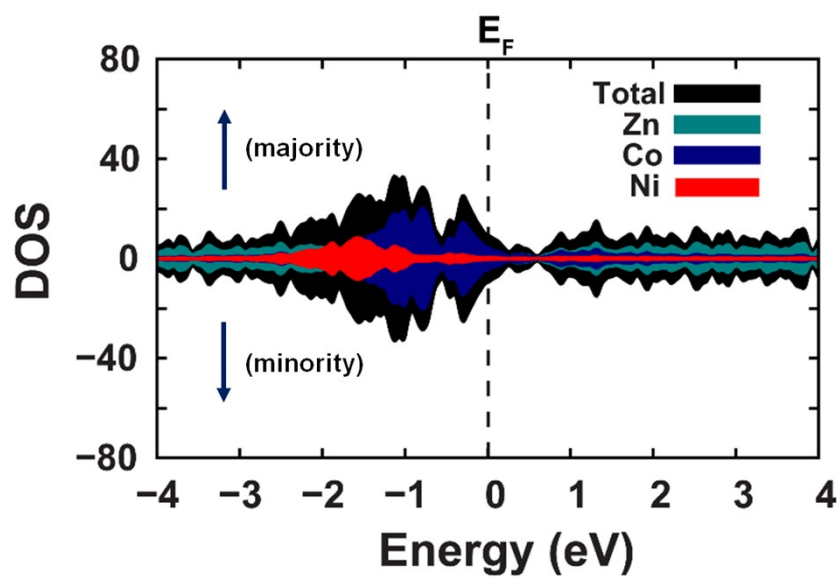


Fig. S7. DOS curve (majority and minority spin) of $\text{Co}_{1.5}\text{Ni}_{0.5}\text{Zn}_{11}$ pseudo-binary γ -brass compound in the Co–Ni–Zn system.

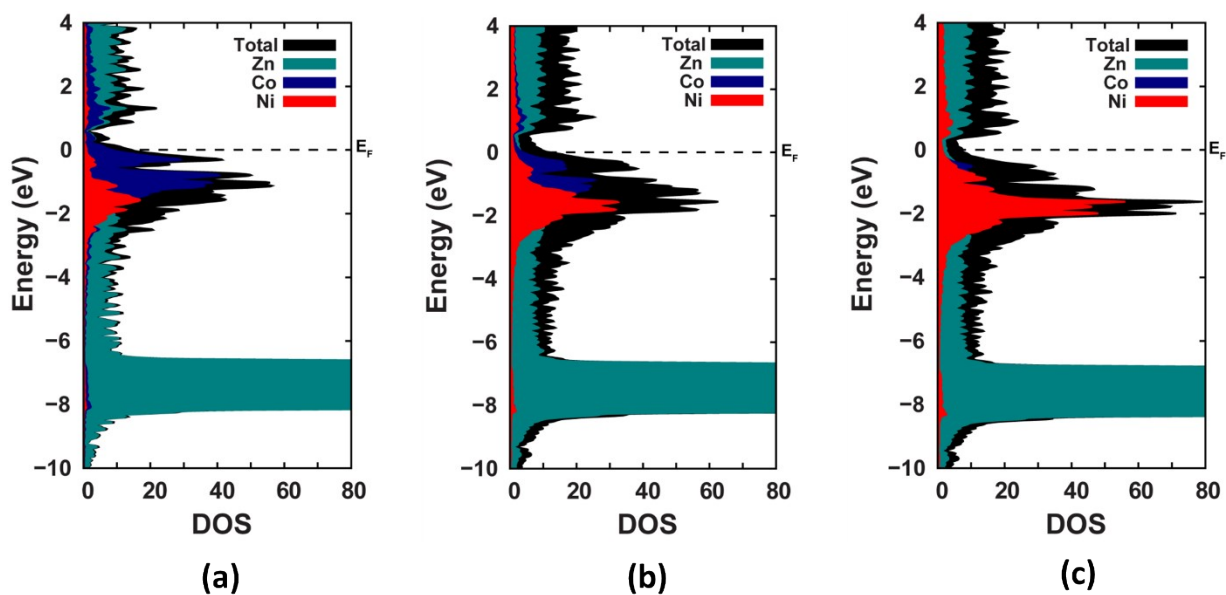


Fig. S8. DOS curves with the energy scale of -10 to $+4$ eV for (a) $\text{Co}_{1.5}\text{Ni}_{0.5}\text{Zn}_{11}$, (b) $\text{Co}_{1.0}\text{Ni}_{1.0}\text{Zn}_{11}$, and (c) $\text{Co}_{0.5}\text{Ni}_{1.5}\text{Zn}_{11}$.

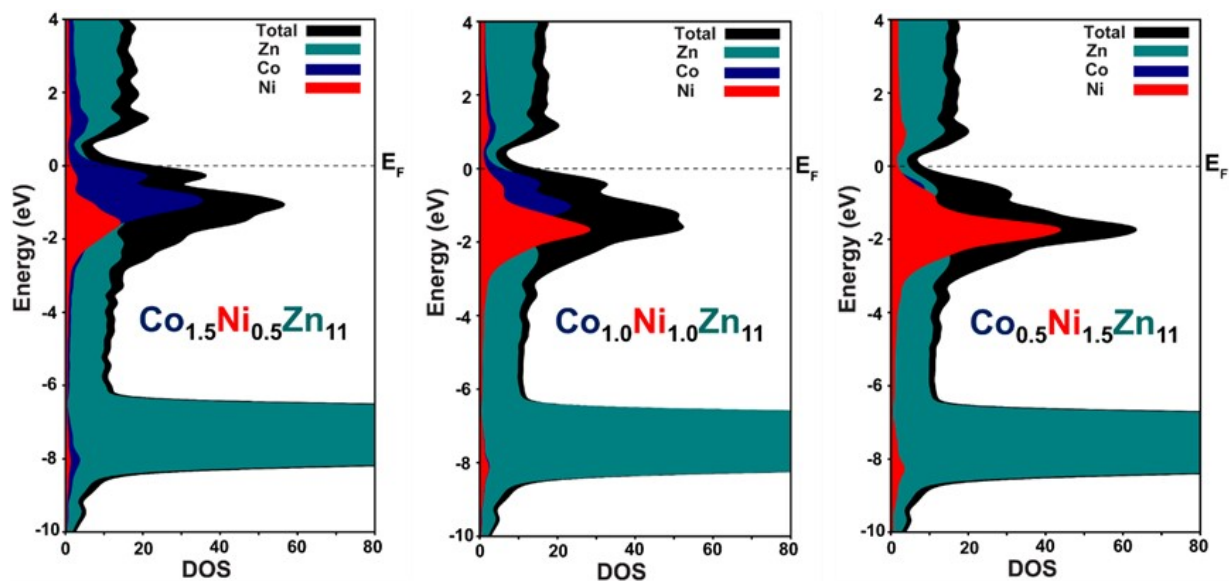


Fig. S9. Representation of total DOS by LOBSTER with the atom projected DOS: (left) “OT model” for $\text{Co}_{1.5}\text{Ni}_{0.5}\text{Zn}_{11}$, (middle) “OT model” for $\text{Co}_{1.0}\text{Ni}_{1.0}\text{Zn}_{11}$, and (right) “OT model” for $\text{Co}_{0.5}\text{Ni}_{1.5}\text{Zn}_{11}$.

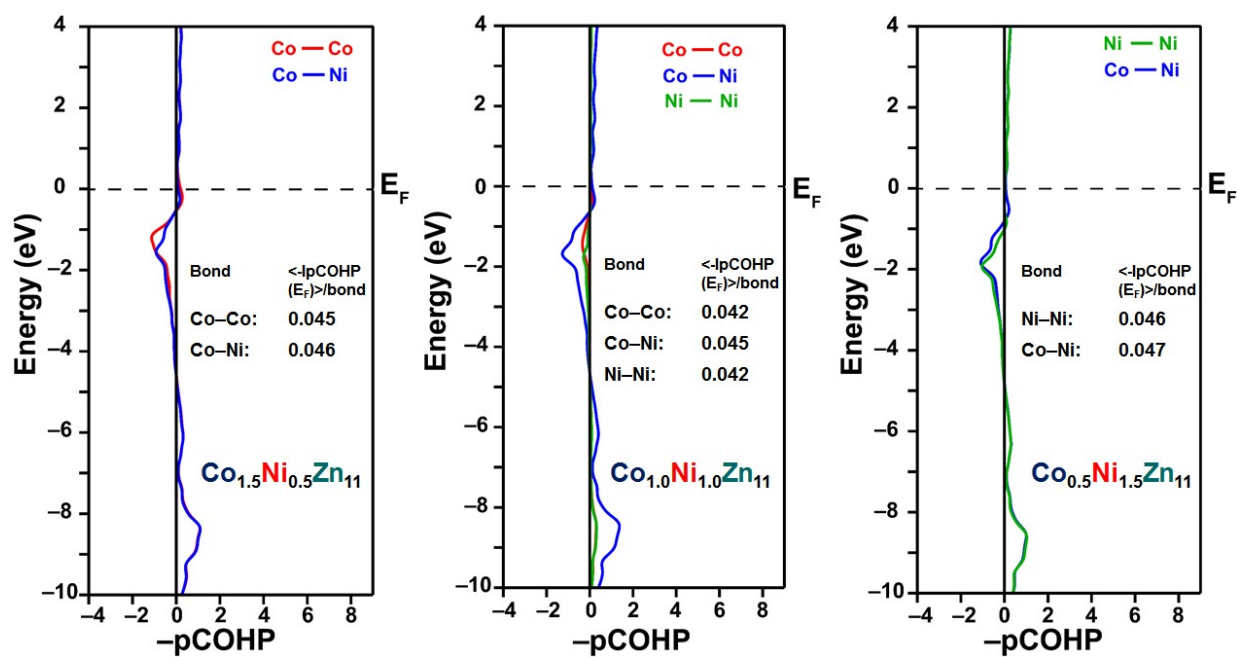


Fig. S10. COHP curves of OT—OT contacts for $\text{Co}_{1.5}\text{Ni}_{0.5}\text{Zn}_{11}$ (left), $\text{Co}_{1.0}\text{Ni}_{1.0}\text{Zn}_{11}$ (middle), and $\text{Co}_{0.5}\text{Ni}_{1.5}\text{Zn}_{11}$ (right).

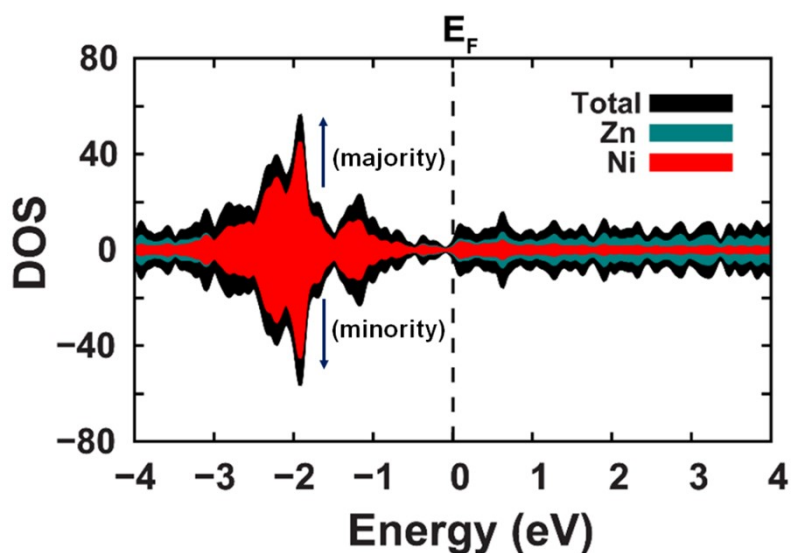


Fig. S11. DOS curve (majority and minority spin) of $\text{Ni}_2\text{Zn}_{11}$ γ -brass compound.

Table S2. Interatomic distances and coordination polyhedron ($< 3.5 \text{ \AA}$) concerning each independent site of $\text{Co}_{1.1}\text{Ni}_{0.9}\text{Zn}_{11}$ compound.

Central atom	Atoms	Interatomic distance (\AA)
Zn1 (IT)	3 Zn2	2.6051(6)
	3 Zn3	2.6137(5)
	3 Co/Ni	2.6239(6)
	3 Zn1	2.6425(6)
	Co/Ni	3.4800(6)
Co1/Ni1 (OT)	3 Zn3	2.5429(5)
	3 Zn3	2.5942(5)
	3 Zn1	2.6239(6)
	3 Zn2	2.7281(5)
	1 Zn1	3.4800(6)
Zn2 (OH)	2 Zn1	2.6051(6)
	1 Zn2	2.6160(8)
	2 Zn3	2.6196(4)
	2 Co/Ni	2.7281(5)
	4 Zn3	2.8107(5)
	2 Zn3	3.0065(5)
Zn3 (CO)	1 Co/Ni	2.5429(6)
	1 Co/Ni	2.5942(5)

1 Zn1	2.6137(5)
1 Zn2	2.6196(5)
4 Zn3	2.7241(5)
2 Zn2	2.8107(4)
1 Zn2	3.0065(5)
2 Zn3	3.2948(5)

Table S3. Site distribution of atoms in a 26-atom γ -

Composition of the model	IT (8c)	OT (8c)	OH (12e)	CO (24g)
Co _{1.5} Ni _{0.5} Zn ₁₁	4Zn	3Co+1Ni	6Zn	12Zn
Co _{1.0} Ni _{1.0} Zn ₁₁	4Zn	2Co+2Ni	6Zn	12Zn
Co _{0.5} Ni _{1.5} Zn ₁₁	4Zn	1Co+3Ni	6Zn	12Zn

cluster for each composition.

Section S1.

The formation energies for the model with composition Co_{2-x}Ni_xZn₁₁ have been evaluated using the following equation,

$$E_{\text{Formation}} = E_{\text{Total}} - Z \times [\{(2-x) \times E_{\text{Co}}\} + \{x \times E_{\text{Ni}}\} + \{11 \times E_{\text{Zn}}\}]$$

Where $E_{\text{Formation}}$ is the formation energy for the respective model. E_{Total} is the calculated total energy. Z is the formula unit (for γ -brass type phase, $Z = 4$). E_{Co} , E_{Ni} , and E_{Zn} are the total energies per atom for Co, Ni, and Zn respectively calculated using the stable allotropes of respective elements *e.g.* f.c.c. phase for Ni and the hexagonal phase for both Co and Zn.

